

# Inhibition of *Acinetobacter baumannii*, *Staphylococcus aureus* and *Pseudomonas aeruginosa* biofilm formation with a class of TAGE-triazole conjugates†

Robert W. Huigens III, Steven A. Rogers, Andrew T. Steinhauer and Christian Melander\*

Received 13th October 2008, Accepted 20th November 2008

First published as an Advance Article on the web 12th January 2009

DOI: 10.1039/b817926c

A chemically diverse library of TAGE-triazole conjugates was synthesized utilizing click chemistry on the TAGE scaffold. This library of small molecules was screened for anti-biofilm activity and found to possess the ability of inhibiting biofilm formation against *Acinetobacter baumannii*, *Staphylococcus aureus* and *Pseudomonas aeruginosa*. One such compound in this library demonstrated the most potent inhibitory effect against *Staphylococcus aureus* biofilm formation that has been displayed by any 2-aminoimidazole derivative.

## Introduction

Recent findings in biomedical research have revealed that biofilm-mediated infections play a prominent role in infectious disease.<sup>1</sup> Bacterial biofilms are defined as highly structured communities of microbial cells attached to a surface and encased in a protective matrix made primarily of polysaccharide material.<sup>2</sup> Biofilm formation occurs when free-swimming planktonic cells collectively coordinate their behavior through a communication pathway involving signaling molecules, termed quorum sensing, resulting in their attachment to a surface and colonization.<sup>3–5</sup> Once a biofilm is established, these bacteria act as if they were a multicellular organism resulting in the virulent phenotypes associated with various biofilm-mediated diseases. Despite their prevalence, biofilm-associated infections have been a medical obstacle due to their increased resistance to conventional antibiotics as well as host immune responses.<sup>6</sup>

There have been relatively few small molecules identified that possess anti-biofilm activity, with anti-biofilm activity defined as modulating biofilm development through non-toxic mechanisms. Examples of compounds possessing anti-biofilm activity include derivatives of homoserine lactones,<sup>7</sup> which are endogenous signaling molecules used by bacteria in quorum sensing,<sup>8,9</sup> brominated furanones which are natural products isolated from the macroalgae *Delisea pulchra*,<sup>10</sup> as well as ursine triterpenes from the plant *Diospyros dendo*.<sup>11</sup> Recently, Junker and Clardy reported the development of a high throughput screen revealing several small molecules capable of inhibiting *Pseudomonas aeruginosa* biofilms (Fig. 1).<sup>12</sup>

Our group has recently developed several novel libraries of 2-aminoimidazole small molecules inspired by the marine alkaloids bromoageliferin **6** and oroidin **10**.<sup>13–19</sup> These natural products were previously reported to inhibit biofilm formation of the marine  $\alpha$ -protobacterium *Rhodospirillum salexigens*.<sup>20</sup> TAGE and CAGE

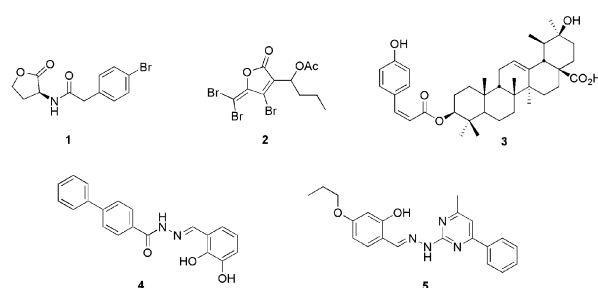


Fig. 1 Previously reported biofilm inhibitors.

were the first documented 2-aminoimidazoles with anti-biofilm activity against *Pseudomonas aeruginosa* biofilms (Fig. 2).<sup>13</sup>

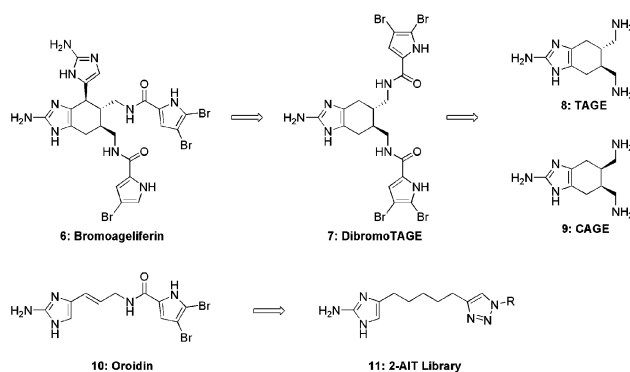


Fig. 2 Representative 2-aminoimidazoles derived from the marine natural products bromoageliferin **6** and oroidin **10**.

Analogs of the structurally simpler alkaloid oroidin were also pursued to develop novel classes of small molecules with anti-biofilm activity. Recently, an oroidin inspired library was constructed utilizing click chemistry to generate a diverse library of 2-aminoimidazole/triazole conjugates (2-AIT). These compounds displayed the widest spectrum of anti-biofilm activity observed within the 2-aminoimidazole class (Fig. 2, **11**).<sup>18</sup>

Based on the potent activity displayed by 2-AIT conjugates, we decided to explore if triazole incorporation within the TAGE scaffold would lead to compounds with enhanced anti-biofilm

North Carolina State University Chemistry Department, 2620 Yarborough Drive, Raleigh, North Carolina, 27695-8204, United States of America

† Electronic supplementary information (ESI) available: Dose-response curves for biofilm inhibition; growth curves at IC<sub>50</sub> value of biofilm inhibition; representative <sup>1</sup>H and <sup>13</sup>C NMR spectra. See DOI: 10.1039/b817926c

activity. To accomplish this goal, we postulated that epoxide **12** could be synthetically elaborated to AzidoTAGE **13** (Fig. 3). The appending azides were designed to serve as synthetic handles for derivatization using click chemistry to generate a TAGE-triazole library.

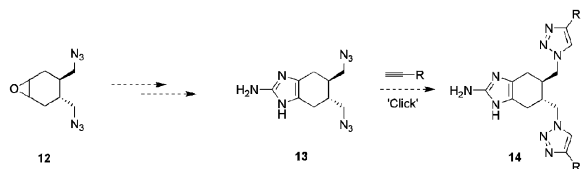
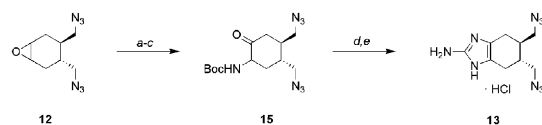


**Fig. 3** Synthetic approach to the construction of a TAGE-triazole library from previously reported epoxide **12**.

## Results and discussion

### Synthesis of TAGE-triazole library

The assembly of the TAGE-triazole library was initiated by refluxing epoxide **12** in a 1:1 mixture of aqueous ammonium hydroxide and methanol saturated with ammonia for 5.5 hours in a sealed tube (Scheme 1). Acid-base extraction yielded the pure aminoalcohol in 97% yield. The resulting amine was then Boc-protected (99% yield) and further subjected to PDC oxidation to give Boc-protected  $\alpha$ -aminoketone **15** in 81% yield. The Boc-group was then removed upon treatment with TFA followed by subsequent addition of HCl in methanol to effect counter ion exchange. This resulting  $\alpha$ -aminoketone  $\cdot$  HCl salt was then dissolved in water followed by the addition of cyanamide and the pH of the solution was adjusted to 4. This reaction was heated to 95 °C for 2.5 hours, delivering AzidoTAGE **13** in 79% yield over 2 steps as the HCl salt.



**Scheme 1** Synthesis of AzidoTAGE **13**. *Reaction conditions:* (a)  $\text{NH}_4\text{OH}$ ,  $\text{H}_2\text{O}$ , MeOH ( $\text{NH}_3$ ), reflux, 97% (b) Boc<sub>2</sub>O, acetone,  $\text{H}_2\text{O}$ ,  $\text{Na}_2\text{CO}_3$ , reflux, 99% (c) PDC, DMF, room temp, 81% (d) TFA,  $\text{CH}_2\text{Cl}_2$ , 0 °C to room temp (e)  $\text{NH}_2\text{CN}$ ,  $\text{H}_2\text{O}$ , pH 4, 95 °C, 79%.

Although this library was designed to combine the 1,2,3-triazole element of the 2-AIT library with the TAGE scaffold,<sup>18</sup> this new platform is chemically distinct from our previous approach to 2-AIT conjugates in that the azides are on the core TAGE scaffold bearing the 2-aminoimidazole. In the 2-AIT library, the terminal alkyne is on the core scaffold with the 2-aminoimidazole. This reversal in click partners allows easier access to a chemically diverse library since most of the azides of the 2-AIT library required synthesis from the corresponding alcohols. The majority of terminal alkynes in this study were commercially available. Alkynes that were not commercially available required only one step and were purified by recrystallization.

The click reaction was carried out in the presence of the HCl salt of AzidoTAGE **13**. The click conditions we employed for this study relied on a 1:1:1 ratio of ethanol:water:dichloromethane, copper

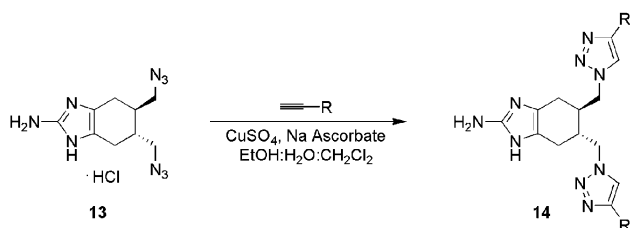
sulfate (15 - 30 mol%) and sodium ascorbate.<sup>18</sup> These reactions were typically carried out overnight at room temperature (16–24 hours). The alkynes chosen for this study vary from being structurally simple hydrocarbon chains to those decorated with brominated pyrrole rings. These TAGE-triazole small molecules provided the necessary diversity to attain a preliminary insight into the SAR of TAGE-triazole conjugates in the context of biofilm inhibition and dispersion. These conditions were shown to be general, allowing the construction of a chemically diverse 21-membered TAGE-triazole library (Table 1). The TAGE-triazole library is composed of four series, which are classified according to the structural variation of the triazole moiety as the hydrocarbon chain series, cycloalkyl series, phenyl series and amide series.

### Biofilm inhibition studies

The TAGE-triazole library was initially screened for anti-biofilm activity against *Acinetobacter baumannii*. *A. baumannii* is a Gram-negative bacterium recognized by the medical field for its role in nosocomial infections. Infections acquired from *A. baumannii* are difficult to treat because they are resistant to many antibiotics, such as penicillin, chloramphenicol and often aminoglycosides.<sup>21</sup> This multidrug-resistance (MDR) is attributed to active drug efflux ability. *A. baumannii* elicits its pathogenicity through biofilm-mediated virulence and tests positive in 25% of all hospital swabs in both the US and Europe.<sup>22,23</sup>

The TAGE-triazole library members were initially screened at 400  $\mu\text{M}$  to eliminate weakly active or inactive TAGE-triazole conjugates. Inhibition screens were run using PVC microtiter plates in a 96-well format. The inside of these wells serves as a surface for biofilm attachment and development during bacterial growth. The amount of biofilm that forms on the inside of these wells is quantified by using a crystal violet reporter assay.<sup>13</sup> These values then serve as a point of comparison to identify lead biofilm inhibitors. This approach quickly eliminated six compounds that were not able to inhibit biofilm formation by 50% at 400  $\mu\text{M}$  (**H5**, **C1**, **P2**, **A1**, **A2**, **A3**). Dose-response curves were then generated for the remaining 15 compounds to determine their respective  $\text{IC}_{50}$  values (Table 2).

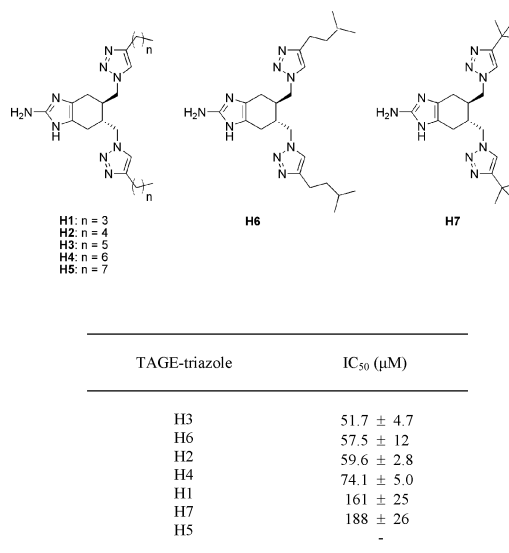
In the series of simple hydrocarbon chains we noted that the inhibitory activity was dependent on chain length and branching (Fig. 4). Using analogue **H1** as our point of reference, extension of the hydrocarbon chain one methylene unit from butyl **H1** to pentyl **H2** increased inhibition activity significantly. The  $\text{IC}_{50}$  of **H1** was measured as  $161 \pm 25 \mu\text{M}$ , while **H2** was  $59.6 \pm 2.8 \mu\text{M}$ . Inhibition activity is increased again by extending the pentyl side chain (**H2**) to the hexyl chain (**H3**). The  $\text{IC}_{50}$  value of **H3** was determined to be  $51.7 \pm 4.7 \mu\text{M}$ . Extending the hydrocarbon chain one more methylene unit from **H3** gave the heptyl derivative **H4** which showed a decrease in activity ( $\text{IC}_{50}$  value of  $74.1 \pm 5.0 \mu\text{M}$ ). Following this structural trend, the decyl side of **H5** showed very weak inhibition activity with only 21% inhibition at 400  $\mu\text{M}$ . Branching of the butyl side chain with the 3-methyl group of **H6** increased the inhibition activity 3-fold compared to the parent butyl chain **H1**. This simple 3-methyl addition to the butyl chain gave an  $\text{IC}_{50}$  value of  $57.5 \pm 12 \mu\text{M}$ . The *t*-butyl side chain of **H7** resulted in a slight decrease of inhibition activity giving an  $\text{IC}_{50}$  value of  $188 \pm 26 \mu\text{M}$ .

**Table 1** Synthesis of the TAGE-triazole library

Series and Terminal Alkyne	% Yield	TAGE-triazole
<b>Hydrocarbon Series (H):</b>		
1-Hexyne	25	<b>H1</b>
1-Heptyne	27	<b>H2</b>
1-Octyne	39	<b>H3</b>
1-Nonyne	32	<b>H4</b>
1-Dodecyne	31	<b>H5</b>
5-Methyl-1-hexyne	64	<b>H6</b>
3,3-Dimethyl-1-butyne	68	<b>H7</b>
<b>Cycloalkyl Series (C):</b>		
Cyclopropylacetylene	27	<b>C1</b>
Cyclopentylacetylene	46	<b>C2</b>
Cyclohexylacetylene	21	<b>C3</b>
3-Cyclopentyl-1-propyne	27	<b>C4</b>
3-Cyclohexyl-1-propyne	35	<b>C5</b>
<b>Phenyl Series (P):</b>		
Phenylacetylene	51	<b>P1</b>
4-Ethynylanisole	47	<b>P2</b>
3-Phenyl-1-propyne	14	<b>P3</b>
4-Phenyl-1-butyne	37	<b>P4</b>
3-Phenoxy-1-propyne	25	<b>P5</b>
<b>Amide Series (A):</b>		
<i>N</i> -(Prop-2-ynyl)benzamide	40	<b>A1</b>
<i>N</i> -(Prop-2-ynyl)-1 <i>H</i> -pyrrole-2-carboxamide	55	<b>A2</b>
4-Bromo- <i>N</i> -(prop-2-ynyl)-1 <i>H</i> -pyrrole-2-carboxamide	14	<b>A3</b>
4,5-Dibromo- <i>N</i> -(prop-2-ynyl)-1 <i>H</i> -pyrrole-2-carboxamide	26	<b>A4</b>

**Table 2** Initial screen of the TAGE-triazole library for biofilm inhibition against *Acinetobacter baumannii* ATCC 19606

TAGE-triazole	% Inhibition at 400 $\mu$ M
<b>H1</b>	83 $\pm$ 3
<b>H2</b>	99 $\pm$ 1
<b>H3</b>	96 $\pm$ 2
<b>H4</b>	98 $\pm$ 1
<b>H5</b>	21 $\pm$ 1
<b>H6</b>	97 $\pm$ 1
<b>H7</b>	76 $\pm$ 9
<b>C1</b>	30 $\pm$ 6
<b>C2</b>	98 $\pm$ 1
<b>C3</b>	99 $\pm$ 1
<b>C4</b>	99 $\pm$ 1
<b>C5</b>	81 $\pm$ 3
<b>P1</b>	70 $\pm$ 7
<b>P2</b>	16 $\pm$ 4
<b>P3</b>	77 $\pm$ 4
<b>P4</b>	98 $\pm$ 1
<b>P5</b>	91 $\pm$ 1
<b>A1</b>	3 $\pm$ 1
<b>A2</b>	7 $\pm$ 2
<b>A3</b>	49 $\pm$ 4
<b>A4</b>	84 $\pm$ 4

**Fig. 4** Structures and biofilm inhibition activity against *A. baumannii* of the TAGE-triazole hydrocarbon chain series.

The cycloalkyl series also provided structural insight into inhibiting *A. baumannii* biofilm formation. We began by determining the activity of the cyclopentyl derivative **C2** which gave an  $IC_{50}$  value of  $79.5 \pm 9.5 \mu\text{M}$ . When a methylene linker was

inserted between the triazole and cyclopentyl ring to give **C4** the activity was essentially identical, giving an  $IC_{50}$  value of  $75.1 \pm 5.7 \mu\text{M}$ . Trading out a 5-membered ring for the 6-membered ring in **C3** gave a slight increase in activity with a measured

IC<sub>50</sub> value of 63.9 ± 5.7 μM. Placement of a methylene spacer between the triazole ring and the cyclohexyl ring (**C5**) greatly reduced inhibition activity as demonstrated by an IC<sub>50</sub> value of 127 ± 14 μM (Fig. 5). Cyclopropyl derivative **C1** demonstrated weak biofilm inhibition activity against *A. baumannii*, inhibiting 30% of biofilm formation at 400 μM.

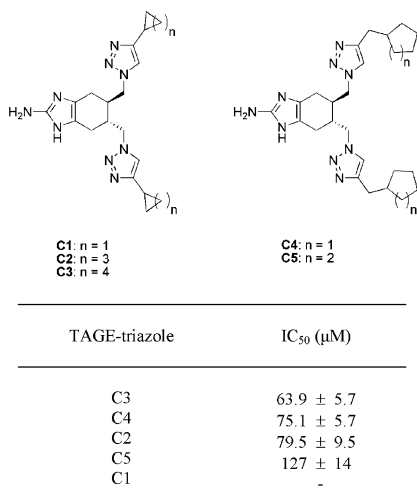


**Fig. 5** Structures and biofilm inhibition activity against *A. baumannii* of the TAGE-triazole cycloalkyl series.

The third class of TAGE-triazoles was based on substituted phenyl derivatives. The phenyl ring derivative **P1** gave an IC<sub>50</sub> value of 120 ± 29 μM against *A. baumannii* biofilm formation. Changing the electronics of the phenyl ring was investigated by adding a 4-methoxy group to the phenyl ring giving **P2**. This greatly decreased the inhibition activity and only 16% biofilm inhibition was observed at 400 μM. Extending the phenyl ring out by adding the methylene unit in **P3** also decreased the activity slightly (IC<sub>50</sub> = 165 ± 12 μM). However, extending the phenyl ring by two methylene units in **P4** greatly increased the activity giving the best inhibitor in the phenyl ring series with an IC<sub>50</sub> value of 61.5 ± 10 μM. Substituting the second methylene unit from the triazole of this active structure with an oxygen atom in **P5** decreased the activity from the lead ethyl spacer within this series by giving an IC<sub>50</sub> value of 80.1 ± 9.5 μM (Fig. 6).

Within the amide series of the TAGE-triazole library, the only active member against *A. baumannii* biofilm formation was **A4** (Fig. 7). The activity of this small molecule was surprising considering the importance of 2-aminoimidazole dibromopyrrole conjugates as biofilm modulators.<sup>14,16,17,19</sup> The IC<sub>50</sub> value for **A4** was determined to be 48.8 ± 8.6 μM. The other members of the amide series demonstrated weak inhibitory activity at 400 μM.

When comparing the relatively complex structure of **A4** to a previous TAGE derivative, DibromoTAGE 7, the inhibition activity drops 3-fold when compared to the previously reported IC<sub>50</sub> value of 15.5 μM against *A. baumannii*.<sup>16</sup> This drop in activity may be attributed to the unoptimized head-to-tail distance from the 2-aminoimidazole head to the dibromopyrrole tail in this structure. Previous studies in our labs have shown that the anti-biofilm activity is dependent on the relative distance between the 2-aminoimidazole moiety and either dibromopyrrole or triazole heterocycles.<sup>17,18</sup>

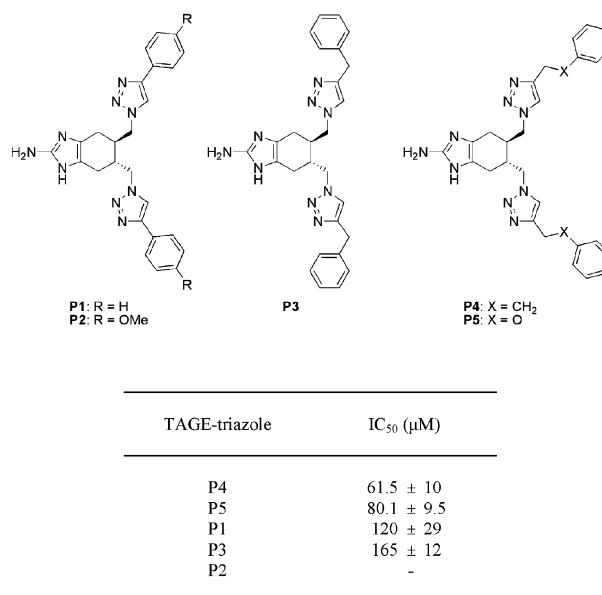


**Fig. 6** Structures and biofilm inhibition activity against *A. baumannii* of the TAGE-triazole phenyl ring series.

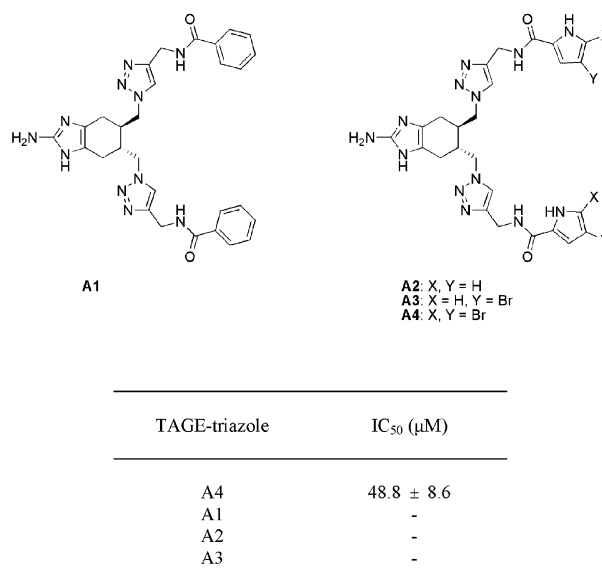


**Fig. 7** Structures and biofilm inhibition activity against *A. baumannii* of the TAGE-triazole amide series.

Each compound that was able to generate an IC<sub>50</sub> value below 400 μM against *A. baumannii* was tested against planktonic bacteria to determine if these small molecules elicited their effects through a toxic mechanism. These compounds were added to a test tube at the IC<sub>50</sub> value and optical densities of the treated and untreated samples were monitored after 1, 3, 5, 7 and 24 hours. After 5 and 7 hours, some TAGE-triazole library members show a slight reduction in the bacterial growth of *A. baumannii*, indicating some bacterial static effects, however, after 24 hours, there was no reduction in the optical densities between treated and untreated planktonic growth.

The next opportunistic bacterium we investigated was *Staphylococcus aureus*, a Gram-positive bacterium responsible for many

**Table 3** Initial screen for biofilm inhibition against *Staphylococcus aureus* ATCC 29213

TAGE-triazole	% Inhibition at 400 $\mu\text{M}$
H1	47 $\pm$ 6
H2	22 $\pm$ 7
H3	93 $\pm$ 1
H4	98 $\pm$ 1
H5	No activity
H6	99 $\pm$ 1
H7	95 $\pm$ 1
C1	No activity
C2	95 $\pm$ 3
C3	71 $\pm$ 5
C4	33 $\pm$ 9
C5	76 $\pm$ 8
P1	22 $\pm$ 1
P2	95 $\pm$ 4
P3	76 $\pm$ 6
P4	97 $\pm$ 2
P5	70 $\pm$ 9
A1	No activity
A2	No activity
A3	No activity
A4	93 $\pm$ 3

nosocomial infections. *S. aureus* is notorious for being multi-drug resistance against several classes of antibiotics (i.e. penicillins, aminoglycosides, glycopeptides). Methicillin-resistant *Staphylococcus aureus* (MRSA) and Vancomycin-resistant *Staphylococcus aureus* (VRSA) are two examples of strains that have developed resistance to conventional antibiotics.<sup>24</sup> Given that *S. aureus* forms robust biofilms, we screened our TAGE-triazoles to identify possible inhibitors of biofilm formation. As with *A. baumannii*, we initially screened this library at 400  $\mu\text{M}$  (Table 3).

From this initial screen eight compounds (**H3**, **H4**, **H6**, **H7**, **C2**, **P2**, **P4**, **A4**) demonstrated greater than 90% inhibition and were further evaluated in inhibition screens. Four of the active TAGE-triazoles were from the hydrocarbon series, one from the cycloalkyl series, two from the phenyl ring series and one from the amide series (Fig. 8).

TAGE-triazole	IC <sub>50</sub> Value
H3	270 $\pm$ 15 $\mu\text{M}$
H4	171 $\pm$ 5 $\mu\text{M}$
H6	224 $\pm$ 15 $\mu\text{M}$
H7	220 $\pm$ 22 $\mu\text{M}$
C2	122 $\pm$ 16 $\mu\text{M}$
P2	118 $\pm$ 13 $\mu\text{M}$
P4	222 $\pm$ 7 $\mu\text{M}$
A4	141 $\pm$ 28 nM

**Fig. 8** IC<sub>50</sub> values for the active TAGE-triazoles against *Staphylococcus aureus*.

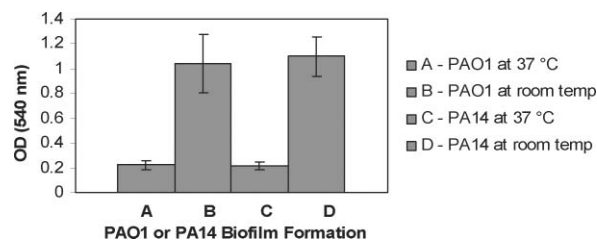
Interestingly **P2**, which showed only 16  $\pm$  4% inhibition at 400  $\mu\text{M}$  against *A. baumannii*, gave 95  $\pm$  4% inhibition at 400  $\mu\text{M}$  against *S. aureus* biofilm formation and upon further evaluation gave an IC<sub>50</sub> value of 118  $\pm$  13  $\mu\text{M}$ . However, when tested for bactericidal activity, growth curves with **P2** indicated a reduction in cellular density of about 25% at the 24 hour time point although there was no reduction during exponential growth. Although several of these compounds were shown to effect bacterial growth

TAGE-triazoles **H7**, **C2**, **P4** and **A4** showed no reduction in bacterial density in the growth curves.

TAGE-triazole **A4** demonstrated the most potent inhibitory effect of any 2-aminoimidazole derivative thus far against *S. aureus* with an IC<sub>50</sub> value of 141  $\pm$  28 nM. We felt that this small molecule would be very effective in inhibition screens since DibromoTAGE 7 was reported to give good inhibition against *S. aureus* (IC<sub>50</sub> value of 14.0  $\mu\text{M}$ ),<sup>16</sup> but some of this activity was occurring by inhibition of bacterial growth. However, the insertion of a triazole moiety adjacent to the dibrominated pyrrole carboxamide not only greatly increases activity (100-fold), but also gives an actual biofilm inhibitor that elicits its anti-biofilm activity through non-toxic means as well as providing the first 2-aminoimidazole with a TAGE scaffold to report an IC<sub>50</sub> value in the nanomolar range.

Finally, we looked to see if this TAGE-triazole library was able to demonstrate anti-biofilm activity against *Pseudomonas aeruginosa*, a Gram-negative, opportunistic bacterium most commonly known for causing morbidity in nearly all those predisposed to the genetic disease that causes cystic fibrosis (CF). This biofilm-forming bacterium is also a threat for infection in burn victims as well as those who are immunocompromised.<sup>25</sup> *P. aeruginosa* is notorious for being multidrug-resistant against many antibiotics as well. There are several mechanisms by which this bacterium evades the action of antimicrobial agents: restricted uptake, multidrug efflux pumps, and the use of chromosomally-encoded antibiotic resistance genes which occur naturally and can be acquired *via* horizontal gene transfer.<sup>26</sup>

During the course of our studies with *P. aeruginosa* we have observed PAO1 and PA14 to be capable of forming a very dense biofilm at room temperature compared to biofilms formed at 37  $^{\circ}\text{C}$  (Fig. 9). Based upon this observation we decided to screen the TAGE-triazole library against PAO1 at room temperature. When inhibition screens are carried out at 37  $^{\circ}\text{C}$ , TAGE 8 was reported to inhibit PAO1 biofilm formation giving an IC<sub>50</sub> value of 100  $\mu\text{M}$ .<sup>13</sup> DibromoTAGE 7 demonstrated a 50-fold increase in biofilm inhibition activity against PAO1 (IC<sub>50</sub> value of 1.77  $\mu\text{M}$ ) compared to TAGE 8.<sup>16</sup>

**Fig. 9** Quantification of biofilm formation by crystal violet staining of microtiter wells at room temperature and 37  $^{\circ}\text{C}$ .

These small molecules were screened at room temperature to demonstrate the difference temperature has on the inhibition of *P. aeruginosa* biofilm formation. TAGE 8 and DibromoTAGE 7 gave IC<sub>50</sub> values of 361  $\pm$  9.5  $\mu\text{M}$  and 15.8  $\pm$  0.7  $\mu\text{M}$  respectively. This is about a 4- to 8-fold higher IC<sub>50</sub> value than those observed at 37  $^{\circ}\text{C}$ . These values correspond to the increase in biofilm formation at room temperature. Based upon this observation, we screened the library at an initial concentration of 500  $\mu\text{M}$  to identify preliminary hits at room temperature.



**Table 4** Biofilm inhibition activity against PAO1 at room temperature

TAGE-triazole	% Inhibition at 500 $\mu$ M
<b>H3</b>	99 $\pm$ 1
<b>C3</b>	96 $\pm$ 1
<b>P1</b>	96 $\pm$ 2
<b>C4</b>	75 $\pm$ 1
<b>H2</b>	62 $\pm$ 5
<b>H6, P5</b>	45 $\pm$ 8
<b>P3</b>	33 $\pm$ 4
<b>C1</b>	28 $\pm$ 9
<b>P4</b>	27 $\pm$ 8
<b>H4</b>	22 $\pm$ 2
<b>A1</b>	20 $\pm$ 5
<b>P2</b>	19 $\pm$ 4
<b>H1, C5, H7</b>	<10
<b>C2, H5, A2, A3, A4</b>	No activity

The results of the initial screen at 500  $\mu$ M are shown in Table 4. Three members of this library (**H3**, **C3**, **P1**) demonstrated >95% inhibitory activity against PAO1 at 500  $\mu$ M. **A4** demonstrated no inhibition activity at 500  $\mu$ M. This was surprising since it closely resembles the structure of DibromoTAGE 7.

We then set out to determine the  $IC_{50}$  value of **H3** against both PAO1 and PA14 with the newly adopted inhibition screen at room temperature to compare this small molecule to TAGE 8 and DibromoTAGE 7. The  $IC_{50}$  values of **H3** were determined to be 98.5  $\pm$  10.9  $\mu$ M and 60.2  $\pm$  2.6  $\mu$ M against PAO1 and PA14 respectively.

TAGE-triazole **H3** was also determined to be acting through a non-toxic mechanism by not killing planktonic bacteria as demonstrated by the growth curves of PAO1 and PA14 after 24 hours. The lead TAGE-triazole **H3** demonstrated inhibition potency against PAO1 and PA14 that was an improvement on that of TAGE 8, however, it does not possess biofilm inhibition activity greater than that of DibromoTAGE 7.

## Conclusions

This novel TAGE-triazole library was constructed utilizing the click reaction to generate a chemically diverse library of small molecules from commercially available or easily prepared terminal alkynes. The implementation of this synthetic route has proven to be an effective approach in generating a chemically diverse set of small molecules possessing structural elements of the biologically active marine alkaloid, bromoageliferin, while tuning the activity with structural variations dictated by the terminal alkyne click partner. Several of these TAGE-triazole compounds were shown to be capable of inhibiting the formation of *A. baumannii*, *S. aureus* and *P. aeruginosa* biofilms. TAGE-triazole **A4** has demonstrated the most potent inhibitory response reported thus far against *S. aureus* biofilm formation. Further developments concerning TAGE-triazole small molecules are underway in our labs and will be reported in due course.

## Experimental

### Biofilm screening

TAGE-triazole library members were dissolved in DMSO, filtered through Whatman 13 mm GD/X syringe filters and stored as

either 50 or 100 mM solutions at  $-20^{\circ}\text{C}$  until needed for biological study. The DMSO used in these biofilm inhibition screens did not exceed 1% by volume and had no effect on bacterial growth or biofilm formation. *Acinetobacter baumannii* and *Staphylococcus aureus* were purchased from ATCC. *Pseudomonas aeruginosa* strains PAO1 and PA14 were donated by Dr. Daniel Wozniak at Wake Forest University School of Medicine.

*A. baumannii* (ATCC 19606) was grown in LB media during the course of this study for inhibition assays and analysis of growth curves. *S. aureus* (ATCC 29213) was grown in Tryptic Soy Broth supplemented with 0.3% glucose. PAO1 and PA14 utilized LBNS (LB "No Salt") as the media for this study.

### Static biofilm inhibition assay

An overnight culture of bacterial strain was subcultured at an  $OD_{600}$  of 0.01 into the media used depending on bacterial strain. This was pipetted into test tubes along with a predetermined concentration of the compound tested. The contents of the test tubes were then poured into tilted Petri dishes and 100  $\mu$ L of medium, bacteria and compound were then transferred into 96-well PVC microtiter plates. These microtiter plates were then covered with a plastic lid, wrapped in Saran wrap and incubated at either room temperature or  $37^{\circ}\text{C}$  for 24 hours. After incubation, the medium was discarded and the plates were vigorously washed twice with water. The remaining biofilm that formed during incubation was stained with 100  $\mu$ L of a 0.1% crystal violet solution and allowed to sit at room temperature for 30 minutes. After 30 minutes, the crystal violet was discarded and washed thoroughly again with water. The remaining crystal violet which stained the biofilm on the inside of the wells was solubilized with 200  $\mu$ L of 95% ethanol. The quantification of biofilm formation was accomplished by transferring 125  $\mu$ L of the ethanol solution into a polystyrene microtiter dish, which was read by spectrophotometry ( $A_{540}$ ). After subtracting the background from each row, a percent inhibition could be calculated by dividing the amount of crystal violet stain in the wells that contained compound by the amount of crystal violet stain in wells that contained bacteria only. Each concentration reported during the course of this study was repeated two to four times with each biofilm inhibition assay being done in 6 or 8 replicates each. The inhibition effectiveness was plotted to generate a 5 to 8 point curve of the percent inhibition of biofilm formation *versus* the concentration of compound tested. This curve was used to determine  $IC_{50}$  values.

### Growth curves

An overnight culture of bacterial strain was subcultured into its respective media at an  $OD_{600}$  of 0.01. The inoculated media (3 ml) was added to two test tubes, one that would not be treated, to serve as a control for bacterial growth, and one that would be treated with a member of the TAGE-triazole library at the  $IC_{50}$  value. The test tubes were shaken while incubated and bacterial growth was monitored at 1, 3, 5, 7 and 24 hours. These experiments were done from three different overnight cultures from three different bacterial colonies in single replicate.

Note: *A. baumannii* and *S. aureus* strains were shaken at 200 rpm at 37 °C in their respective media. PAO1 and PA14 were agitated at 350 rpm at room temperature in LBNS.

## Chemistry

All chemicals and solvents used for the chemical synthesis of the TAGE-triazole library were purchased from commercially available sources and used without further purification. Silica gel was used for column chromatography and was performed with 60 Å mesh standard grade silica gel from Sorbtech. <sup>1</sup>H and <sup>13</sup>C NMR spectra were performed using Varian 300 MHz and 400 MHz spectrometers. Chemical shifts are reported in parts per million relative to CDCl<sub>3</sub> (δ 7.26), CD<sub>3</sub>OD (δ 4.78 or 3.31) and DMSO-*d*<sub>6</sub> (δ 2.50) for <sup>1</sup>H NMR and relative to CDCl<sub>3</sub> (δ 77.23), CD<sub>3</sub>OD (δ 49.51) and DMSO-*d*<sub>6</sub> (δ 39.51) for <sup>13</sup>C NMR with TMS as an internal standard. High-resolution mass spectra were obtained at the North Carolina State Mass Spectrometry Laboratory for Biotechnology.

**trans-2-Amino-trans-4,5-bis(azidomethyl)cyclohexanol.** 2.889 g (13.9 mmol) of epoxide **12** was added to a stirring solution of aqueous NH<sub>4</sub>OH (80 ml) in a sealed tube. Ammonia-saturated methanol (80 ml) was then added to completely dissolve the starting material. The tube was then sealed and refluxed for 5.5 hours. The reaction was then cooled in an ice bath before removal of the seal. The reaction was then concentrated under vacuum pressure to give a dark yellow residue. The resulting amine was purified by acid-base extraction by adding 5% HCl (aq) to the residue. The organic layer was collected and discarded. The acidic aqueous layer was then treated with 10% NaOH (aq) until the aqueous layer was basic and the organic layer was collected, dried with sodium sulfate and concentrated to give 3.024 g (97% yield) of a light yellow residue as a free base of the aminoalcohol product. <sup>1</sup>H NMR (300 MHz, CD<sub>3</sub>OD) δ 3.48 (m, 1H), 3.39 (m, 4H), 3.27 (m, 4H), 2.74 (bs, 1H), 1.93–1.70 (m, 4H), 1.62–1.45 (m, 2H); <sup>13</sup>C NMR (100 MHz, CD<sub>3</sub>OD) δ 71.9, 55.6, 55.5, 52.5, 36.3, 35.7, 32.4, 31.8; HRMS (ESI) calculated for C<sub>8</sub>H<sub>16</sub>N<sub>7</sub>O (MH<sup>+</sup>) 226.1410, found 226.1409.

**tert-Butyl-trans-4,5-bis(azidomethyl)-2-hydroxycyclohexylcarbamate.** Di-*tert*-butyl dicarbonate (4.392 g, 20.1 mmol) was added to a stirred solution of 3.024 g (13.5 mmol) of the aminoalcohol product from the previous step in acetone (50 ml) and distilled water (30 ml). Then 4.951 g of sodium carbonate (46.7 mmol) was added and the reaction was refluxed for 1 hour. The reaction was quenched with brine and upon cooling the reaction was added to a separatory funnel and extracted with ethyl acetate. The organic layer was washed two times with brine and collected. After drying the organic layer with sodium sulfate the organic layer was concentrated to give 4.355 g (99% yield) of the Boc-protected aminoalcohol as a yellow oil which required no further purification. <sup>1</sup>H NMR (300 MHz, CDCl<sub>3</sub>) δ 4.83 (bs, 1H), 3.76 (m, 1H), 3.61 (m, 1H), 3.44–3.25 (m, 4H) 1.92–1.82 (m, 2H), 1.63–1.46 (m, 4H), 1.39 (s, 9H); <sup>13</sup>C NMR (75 MHz, CD<sub>3</sub>Cl) δ 155.9, 79.9, 67.9, 54.4, 54.3, 34.3, 33.7, 31.6, 29.0, 28.4, 27.3; HRMS (ESI) calculated for C<sub>13</sub>H<sub>23</sub>N<sub>7</sub>O<sub>3</sub>Na (MNa<sup>+</sup>) 348.1754, found 348.1754.

**tert-Butyl-trans-4,5-bis(azidomethyl)-2-oxocyclohexylcarbamate (15).** 404 mg (1.24 mmol) of the Boc-protected aminoal-

cohol synthesized in the previous step was dissolved in 12 ml DMF. PDC (2.867 g, 7.63 mmol) was then added and the reaction was allowed to stir at room temperature for 24 hours. The reaction was quenched with brine and extracted with ethyl acetate. The organic layer was then washed two times with brine. Sodium sulfate was added to dry the organic layer. Then the organic layer was concentrated and purified by flash column chromatography using 5:1 hexanes:ethyl acetate to afford 328 mg (81% yield) of **15** inseparable epimers as a clear oil. <sup>1</sup>H NMR (300 MHz, CDCl<sub>3</sub>) δ 5.47–5.35 (m, 1H), 4.23 (m, 1H), 3.61 (m, 1H), 3.52–3.24 (m, 3H), 2.61–2.50 (m, 1H), 2.49–2.34 (m, 2H), 2.09 (m, 1H), 1.94 (m, 1H), 1.73–1.68 (m, 1H), 1.43 (s, 9H); <sup>13</sup>C NMR (75 MHz, CD<sub>3</sub>Cl) δ 205.9, 205.2, 155.2, 79.9, 77.4, 57.9, 55.2, 54.1, 53.8, 53.4, 53.1, 43.3, 40.5, 39.5, 38.4, 37.9, 37.0, 34.8, 33.1, 28.4, 28.3, 27.7; HRMS (ESI) calculated for C<sub>13</sub>H<sub>21</sub>N<sub>7</sub>O<sub>3</sub>Na (MNa<sup>+</sup>) 323.1706, found 323.1713.

**AzidoTAGE (13).** To a stirred solution of **15** (437 mg, 1.34 mmol) in methylene chloride was added 4 ml of TFA dropwise at 0 °C. The reaction continued to stir at 0 °C for one hour and then was allowed to warm to room temperature for an additional one hour. The reaction was then concentrated and a solution of HCl in methanol was added and concentrated overnight. Distilled water was added (8 ml) and a 50% cyanamide solution (50% by weight, 500 mg) was added to the residue and heated to 95 °C for 2.5 hours. The pH was 4 for this reaction and required no additional adjustments. The reaction was then allowed to cool and ethanol was added to assist the concentration of this aqueous mixture under high vacuum pressure. It was necessary to wash the residue with ether (2 × 150 ml) before column chromatography. **AzidoTAGE (13)** was purified by flash column chromatography using 10% methanol/ammonia in methylene chloride to afford an orange foam. After 48 hours on a high vacuum pump to remove all residual ammonia, **13** was then acidified using HCl in methanol to give 304 mg (79% yield) as a light yellow foam. <sup>1</sup>H NMR (400 MHz, DMSO-*d*<sub>6</sub>) δ 11.75 (s, 2H), 7.42 (s, 2H), 3.55–3.38 (m, 4H), 2.29 (m, 2H), 2.24 (m, 2H), 2.02 (m, 2H); <sup>13</sup>C NMR (100 MHz, CD<sub>3</sub>OD) δ 148.4, 119.8, 54.6, 36.5, 23.2; HRMS (ESI) calculated for C<sub>9</sub>H<sub>14</sub>N<sub>9</sub> (MH<sup>+</sup>) 248.1366, found 248.1365.

## General procedure for click reaction

To a vial with 60–80 mg of AzidoTAGE·HCl was added 1 ml of ethanol, 1 ml of distilled water and 1 ml of methylene chloride. A stir bar was added and the mixture was stirred to dissolve the starting AzidoTAGE·HCl. Then 6 to 15 equivalents of the predetermined alkyne were added to the reaction mixture. Then 30 to 60 mol% of sodium ascorbate relative to the alkyne was added and allowed to dissolve. Finally CuSO<sub>4</sub> was added to the reaction mixture and the reaction stirred overnight (16–24 hours). The reaction was stopped by adding methanol and transferring to a round bottom flask where the contents were concentrated under high pressure vacuum and the resulting residue was purified by flash column chromatography using 1:15 methanol/NH<sub>3</sub>:methylene chloride as the solvent and increasing the methanol/NH<sub>3</sub> gradually to 1:4 until the purified TAGE-triazole analogue was collected as the free base.

**(H1.) Butyl TAGE-triazole.** <sup>1</sup>H NMR (300 MHz, CD<sub>3</sub>OD) δ 7.70 (s, 2H), 4.42 (m, 4H), 2.69 (t, *J* = 7.2 Hz, 6H), 2.35–2.21

(m, 4H), 1.64 (quintet,  $J = 7.5$  Hz, 4H), 1.35 (sextet,  $J = 7.4$  Hz, 4H), 0.95 (t,  $J = 7.5$ , 6H);  $^{13}\text{C}$  NMR (300 MHz,  $\text{CD}_3\text{OD}$ )  $\delta$  154.0, 149.9, 123.7, 120.1, 53.1, 37.2, 32.8, 26.1, 23.3, 21.8, 14.1; HRMS (ESI) calculated for  $\text{C}_{21}\text{H}_{33}\text{N}_9$  ( $\text{MH}^+$ ) 412.2931, found 412.2930.

**(H2.) Pentyl TAGE-triazole.**  $^1\text{H}$  NMR (300 MHz,  $\text{CD}_3\text{OD}$ )  $\delta$  7.71 (s, 2H), 4.44 (m, 4H), 2.68 (t,  $J = 7.8$  Hz, 6H), 2.38 (m, 2H), 2.28 (s, 1H), 2.23 (s, 1H), 1.64 (quintet,  $J = 7.5$  Hz, 4H), 1.33 (m, 8H), 0.92 (t,  $J = 7.1$  Hz, 6H);  $^{13}\text{C}$  NMR (100 MHz,  $\text{CD}_3\text{OD}$ )  $\delta$  149.8, 149.3, 123.8, 119.3, 52.9, 36.9, 32.6, 30.4, 26.4, 23.6, 21.1, 14.5; HRMS (ESI) calculated for  $\text{C}_{23}\text{H}_{38}\text{N}_9$  ( $\text{MH}^+$ ) 439.3172, found 439.3162.

**(H3.) Hexyl TAGE-triazole.**  $^1\text{H}$  NMR (300 MHz,  $\text{CD}_3\text{OD}$  at 4.78 ppm)  $\delta$  7.63 (s, 2H), 4.37 (m, 4H), 2.61 (m, 6H), 2.28 (s, 2H), 2.20 (s, 1H), 2.14 (s, 1H), 1.56 (m, 4H), 1.27 (m, 12H), 0.83 (m, 6H);  $^{13}\text{C}$  NMR (75 MHz,  $\text{CD}_3\text{OD}$ )  $\delta$  151.2, 149.7, 123.7, 122.2, 53.5, 37.6, 32.8, 30.6, 30.0, 26.5, 23.7, 23.0, 14.4; HRMS (ESI) calculated for  $\text{C}_{25}\text{H}_{42}\text{N}_9$  ( $\text{MH}^+$ ) 468.3557, found 468.3550.

**(H4.) Heptyl TAGE-triazole.**  $^1\text{H}$  NMR (300 MHz,  $\text{CD}_3\text{OD}$ )  $\delta$  7.70 (s, 2H), 4.41 (m, 4H), 2.67 (m, 6H), 2.35 (m, 2H), 2.27 (s, 1H), 2.21 (m, 1H), 1.66 (m, 4H), 1.35–1.30 (m, 18H), 0.90 (m, 6H);  $^{13}\text{C}$  NMR (75 MHz,  $\text{CD}_3\text{OD}$ )  $\delta$  149.6, 124.0, 123.9, 123.7, 53.5, 37.5, 33.1, 30.7, 30.4, 30.3, 26.4, 23.8, 22.9, 14.6; HRMS (ESI) calculated for  $\text{C}_{27}\text{H}_{46}\text{N}_9\text{Na}$  ( $\text{MNa}^+$ ) 495.3798, found 495.3805.

**(H5.) Decyl TAGE-triazole.**  $^1\text{H}$  NMR (300 MHz,  $\text{CD}_3\text{OD}$  at 4.78 ppm)  $\delta$  7.61 (s, 2H), 4.35 (m, 4H), 2.60 (m, 6H), 2.25–2.13 (m, 4H), 1.58 (m, 4H), 1.25 (m, 28H), 0.82 (t,  $J = 6.6$ , 6H);  $^{13}\text{C}$  NMR (75 MHz,  $\text{CD}_3\text{OD}$ )  $\delta$  151.3, 149.7, 123.7, 122.2, 53.5, 37.5, 33.2, 30.8, 30.8, 30.7, 30.6, 30.5, 30.4, 26.4, 23.8, 22.9, 14.5; HRMS (ESI) calculated for  $\text{C}_{33}\text{H}_{58}\text{N}_9$  ( $\text{MH}^+$ ) 580.4809, found 580.4806.

**(H6.) 3-Methylbutyl TAGE-triazole.**  $^1\text{H}$  NMR (300 MHz,  $\text{CD}_3\text{OD}$  at 4.78 ppm)  $\delta$  7.58 (s, 2H), 4.29 (m, 4H), 2.56 (m, 4H), 2.50 (m, 2H), 2.22 (m, 2H), 2.13 (s, 1H), 2.08 (s, 1H), 1.43 (m, 6H), 0.82 (d,  $J = 3.0$  Hz, 12 H);  $^{13}\text{C}$  NMR (75 MHz,  $\text{CD}_3\text{OD}$ )  $\delta$  151.1, 149.8, 123.6, 122.1, 54.9, 54.6, 39.9, 37.6, 36.7, 28.9, 24.4, 22.9; HRMS (ESI) calculated for  $\text{C}_{23}\text{H}_{37}\text{N}_9$  ( $\text{MH}^+$ ) 439.3172, found 439.3176.

**(H7.) *t*-Butyl TAGE-triazole.**  $^1\text{H}$  NMR (300 MHz,  $\text{CD}_3\text{OD}$  at 3.31 ppm)  $\delta$  7.72 (s, 2H), 4.48–4.34 (m, 4H), 2.68 (m, 1H), 2.63 (m, 1H), 2.36 (m, 2H), 2.27 (s, 1H), 2.21 (s, 1H), 1.33 (s, 18 s);  $^{13}\text{C}$  NMR (75 MHz,  $\text{CD}_3\text{OD}$ )  $\delta$  159.0, 151.0, 121.9, 121.7, 53.4, 37.5, 31.8, 30.8, 22.6; HRMS (ESI) calculated for  $\text{C}_{21}\text{H}_{33}\text{N}_9\text{Na}$  ( $\text{MNa}^+$ ) 434.2751, found 434.2751.

**(C1.) Cyclopropyl TAGE-triazole.**  $^1\text{H}$  NMR (400 MHz,  $\text{CD}_3\text{OD}$  at 3.31 ppm)  $\delta$  7.68 (s, 2H), 4.41 (m, 4H), 2.65 (m, 2H), 2.38–2.22 (m, 4H), 1.96 (m, 2H), 0.96 (m, 4H), 0.77 (m, 4H);  $^{13}\text{C}$  NMR (100 MHz,  $\text{CD}_3\text{OD}$ )  $\delta$  151.9, 150.4, 122.6, 121.0, 53.3, 37.2, 22.2, 8.3, 7.4; HRMS (ESI) calculated for  $\text{C}_{19}\text{H}_{25}\text{N}_9$  ( $\text{MNa}^+$ ) 379.2236, found 379.2233.

**(C2.) Cyclopentyl TAGE-triazole.**  $^1\text{H}$  NMR (300 MHz,  $\text{CD}_3\text{OD}$  at 4.78 ppm)  $\delta$  7.60 (s, 2H), 4.39–4.22 (m, 4H), 3.04 (m, 2H), 2.55 (m, 2H), 2.24 (bm, 2H), 2.16 (m, 1H), 2.11 (m, 1H), 2.01–1.94 (m, 4H), 1.74–1.52 (m, 12H);  $^{13}\text{C}$  NMR (75 MHz,  $\text{CD}_3\text{OD}$ )  $\delta$  154.0, 151.1, 122.7, 122.0, 53.5, 38.0, 37.5, 34.3, 26.2, 22.9; HRMS (ESI) calculated for  $\text{C}_{23}\text{H}_{33}\text{N}_9\text{Na}$  ( $\text{MNa}^+$ ) 458.2751, found 458.2749.

**(C3.) Cyclohexyl TAGE-triazole.**  $^1\text{H}$  NMR (300 MHz,  $\text{CD}_3\text{OD}$  at 3.31 ppm)  $\delta$  7.68 (s, 2H), 4.39 (m, 4H), 2.69–2.64 (m, 4H), 2.27–2.27 (m, 4H), 1.99 (m, 4H), 1.80 (m, 6H), 1.43 (m, 12H);  $^{13}\text{C}$  NMR (75 MHz,  $\text{CD}_3\text{OD}$ )  $\delta$  154.9, 122.8, 122.7, 122.4, 53.4, 37.4, 36.7, 34.3, 27.4, 27.3, 22.6; HRMS (ESI) calculated for  $\text{C}_{25}\text{H}_{38}\text{N}_9$  ( $\text{MH}^+$ ) 463.3172, found 463.3164.

**(C4.) Methylenecyclopentyl TAGE-triazole.**  $^1\text{H}$  NMR (300 MHz,  $\text{CD}_3\text{OD}$  at 3.31 ppm)  $\delta$  7.70 (s, 2H), 4.42 (m, 4H), 2.68 (d,  $J = 7.2$ , 4H), 2.33–2.12 (m, 6H), 1.77–1.53 (m, 14H), 1.29–1.19 (m, 4H);  $^{13}\text{C}$  NMR (100 MHz,  $\text{CD}_3\text{OD}$ )  $\delta$  151.0, 149.1, 124.0, 121.7, 53.4, 41.5, 37.5, 33.5, 32.5, 30.7, 30.6, 27.3, 26.2, 22.7; HRMS (ESI) calculated for  $\text{C}_{25}\text{H}_{38}\text{N}_9$  ( $\text{MH}^+$ ) 463.3172, found 463.3172.

**(C5.) Methylenecyclohexyl TAGE-triazole.**  $^1\text{H}$  NMR (400 MHz,  $\text{CD}_3\text{OD}$  at 3.31 ppm)  $\delta$  7.69 (s, 2H), 4.50–4.36 (m, 4H), 2.65 (m, 4H), 2.56 (d,  $J = 6.8$ , 2H), 2.35–2.24 (m, 4H), 1.70–1.60 (m, 10H), 1.29–1.21 (m, 8H), 1.01–0.93 (m, 4H);  $^{13}\text{C}$  NMR (100 MHz,  $\text{CD}_3\text{OD}$ )  $\delta$  151.0, 148.1, 124.3, 121.8, 53.4, 39.6, 37.5, 34.3, 34.2, 27.6, 27.4, 22.8; HRMS (ESI) calculated for  $\text{C}_{27}\text{H}_{42}\text{N}_9$  ( $\text{MH}^+$ ) 491.3485, found 491.3483.

**(P1.) Phenyl TAGE-triazole.**  $^1\text{H}$  NMR (300 MHz,  $\text{CD}_3\text{OD}$  at 3.31 ppm)  $\delta$  8.37 (s, 2H), 7.80 (d,  $J = 5.1$ , 4H), 7.43 (t,  $J = 5.7$ , 4H), 7.36 (m, 2H), 4.60 (m, 4H), 2.80 (m, 1H), 2.75 (m, 1H), 2.57 (m, 2H), 2.41 (s, 1H), 2.39 (s, 1H);  $^{13}\text{C}$  NMR (75 MHz,  $\text{CD}_3\text{OD}$ )  $\delta$  149.5, 149.2, 131.8, 130.1, 129.6, 126.9, 122.9, 121.7, 53.3, 37.0, 21.4; HRMS (ESI) calculated for  $\text{C}_{25}\text{H}_{26}\text{N}_9$  ( $\text{MH}^+$ ) 452.2305, found 452.2311.

**(P2.) 4-Methoxyphenyl TAGE-triazole.**  $^1\text{H}$  NMR (300 MHz,  $\text{CD}_3\text{OD}$  at 3.31 ppm)  $\delta$  8.26 (s, 2H), 7.71 (d,  $J = 6.3$  Hz, 4H), 6.98 (d,  $J = 6.6$  Hz, 4H), 4.57 (m, 4H), 3.83 (s, 6H), 2.78 (m, 1H), 2.74 (m, 1H), 2.56 (m, 2H), 2.40 (s, 1H), 2.36 (s, 1H);  $^{13}\text{C}$  NMR (100 MHz,  $\text{DMSO}-d_6$ )  $\delta$  162.5, 159.0, 146.3, 126.5, 123.2, 121.1, 117.0, 114.3, 55.2, 51.2, 34.8, 19.7; HRMS (ESI) calculated for  $\text{C}_{27}\text{H}_{30}\text{N}_9\text{O}_2$  ( $\text{MH}^+$ ) 512.2516, found 512.2520.

**(P3.) Methylphenyl TAGE-triazole.**  $^1\text{H}$  NMR (300 MHz,  $\text{CD}_3\text{OD}$  at 3.31 ppm)  $\delta$  7.64 (s, 2H), 7.29–7.16 (m, 10H), 4.44–4.31 (m, 4H), 4.02 (s, 4H), 2.63 (m, 1H), 2.59 (m, 1H), 2.32 (m, 2H), 2.22 (s, 1H), 2.18 (s, 1H);  $^{13}\text{C}$  NMR (75 MHz,  $\text{CD}_3\text{OD}$ )  $\delta$  151.1, 148.8, 140.6, 129.8, 129.7, 127.7, 124.4, 121.8, 53.5, 37.4, 32.7, 22.6; HRMS (ESI) calculated for  $\text{C}_{27}\text{H}_{30}\text{N}_9\text{O}_2$  ( $\text{MH}^+$ ) 479.2546, found 479.2545.

**(P4.) Ethylphenyl TAGE-triazole.**  $^1\text{H}$  NMR (300 MHz,  $\text{CD}_3\text{OD}$  at 3.31 ppm)  $\delta$  7.49 (s, 2H), 7.49–7.19 (m, 4H), 7.14 (m, 6H), 4.37 (m, 4H), 2.97 (m, 8H), 2.60 (m, 1H), 2.56 (m, 1H), 2.21–2.16 (m, 4H);  $^{13}\text{C}$  NMR (75 MHz,  $\text{CD}_3\text{OD}$ )  $\delta$  150.7, 148.7, 142.4, 129.7, 129.5, 127.3, 124.1, 121.6, 53.3, 37.3, 36.7, 28.3, 22.7; HRMS (ESI) calculated for  $\text{C}_{29}\text{H}_{34}\text{N}_9$  ( $\text{MH}^+$ ) 508.2931, found 508.2923.

**(P5.) Methylenephenoxy TAGE-triazole.**  $^1\text{H}$  NMR (300 MHz,  $\text{CD}_3\text{OD}$  at 3.31 ppm)  $\delta$  8.00 (s, 2H), 7.26 (m, 4H), 6.99–6.92 (m, 6H), 5.14 (s, 4H), 4.46 (m, 4H), 2.66 (m, 2H), 2.36 (m, 2H), 2.27 (s, 1H), 2.23 (s, 1H);  $^{13}\text{C}$  NMR (100 MHz,  $\text{CD}_3\text{OD}$ )  $\delta$  165.8, 164.6, 159.9, 145.5, 130.7, 125.9, 122.5, 116.2, 62.6, 53.6, 37.4, 22.7; HRMS (ESI) calculated for  $\text{C}_{27}\text{H}_{28}\text{N}_9\text{O}_2$  ( $\text{MH}^+$ ) 510.2366, found 510.2347.



**(A1.) Phenylamide TAGE-triazole.**  $^1\text{H}$  NMR (400 MHz,  $\text{CD}_3\text{OD}$  at 3.31 ppm)  $\delta$  7.90 (s, 2H), 7.83 (d,  $J = 7.2$ , 4H), 7.50 (t,  $J = 7.4$ , 2H), 7.42 (t,  $J = 7.4$ , 4H), 4.61 (s, 4H), 4.48–4.34 (m, 4H), 2.59 (bm, 2H), 2.36 (bm, 2H), 2.24 (bm, 1H), 2.20 (bm, 1H);  $^{13}\text{C}$  NMR (100 MHz,  $\text{CD}_3\text{OD}$ )  $\delta$  170.2, 150.3, 146.8, 135.4, 133.0, 129.7, 128.5, 125.0, 120.9, 53.3, 37.2, 36.3, 22.2 HRMS (ESI) calculated for  $\text{C}_{29}\text{H}_{32}\text{N}_{11}\text{O}_2$  ( $\text{MH}^+$ ) 565.2661, found 565.2661.

**(A2.) Pyrrole TAGE-triazole.**  $^1\text{H}$  NMR (300 MHz,  $\text{CD}_3\text{OD}$  at 3.31 ppm)  $\delta$  7.86 (s, 2H), 6.90 (s, 2H), 6.82 (d,  $J = 2.7$  Hz, 2H), 6.13 (t,  $J = 3.2$  Hz, 2H), 4.56 (s, 4H), 4.46–4.37 (m, 4H), 2.57 (m, 2H), 2.36 (bm, 2H), 2.25 (bm, 1H), 2.19 (bm, 1H);  $^{13}\text{C}$  NMR (75 MHz,  $\text{CD}_3\text{OD}$ )  $\delta$  163.8, 149.1, 147.3, 126.7, 125.0, 123.4, 119.2, 112.5, 110.5, 53.0, 36.8, 35.6, 21.2; HRMS (ESI) calculated for  $\text{C}_{25}\text{H}_{30}\text{N}_{13}\text{O}_2$  ( $\text{MH}^+$ ) 543.2567, found 543.2560.

**(A3.) Bromopyrrole TAGE-triazole.**  $^1\text{H}$  NMR (400 MHz,  $\text{CD}_3\text{OD}$  at 3.31 ppm)  $\delta$  7.91 (s, 2H), 6.93 (s, 2H), 6.81 (s, 2H), 4.57 (s, 4H), 4.56–4.35 (m, 4H), 2.65 (bm, 2H), 2.42 (bm, 2H), 2.31 (m, 1H), 2.27 (m, 1H);  $^{13}\text{C}$  NMR (100 MHz,  $\text{CD}_3\text{OD}$ )  $\delta$  162.6, 148.9, 147.1, 127.4, 125.1, 123.2, 119.0, 113.9, 97.7, 53.0, 36.7, 35.7, 21.1; HRMS (ESI) calculated for  $\text{C}_{25}\text{H}_{27}\text{N}_{13}\text{O}_2\text{Br}_2\text{Na}$  ( $\text{MNa}^+$ ) 722.0675, found 722.0669.

**(A4.) Dibromopyrrole TAGE-triazole.**  $^1\text{H}$  NMR (400 MHz,  $\text{CD}_3\text{OD}$  at 3.31 ppm)  $\delta$  7.93 (s, 2H), 6.86 (s, 2H), 4.56 (s, 4H), 4.55–4.40 (m, 4H), 2.65 (m, 2H), 2.41 (bm, 2H), 2.28 (bm, 2H);  $^{13}\text{C}$  NMR (100 MHz,  $\text{CD}_3\text{OD}$ )  $\delta$  161.8, 149.0, 147.0, 128.7, 125.0, 119.1, 114.9, 106.5, 100.2, 53.0, 36.8, 35.8, 21.2; HRMS (ESI) calculated for  $\text{C}_{25}\text{H}_{26}\text{N}_{13}\text{O}_2\text{Br}_4$  ( $\text{MH}^+$ ) 855.9060, found 855.9035.

***N*-(Prop-2-ynyl)benzamide.** This compound has been previously reported. For this study it was synthesized in accordance with the procedure in ref. 27.

#### General procedure for acylation of propargyl amine with pyrrole derivatives

Propargyl amine (300  $\mu\text{L}$ ) was added to a stirring solution of the desired 2-(trichloroacetyl)-pyrrole (0.95 equiv) with  $\text{Na}_2\text{CO}_3$  (3 equiv) in methylene chloride at room temperature. The reaction was allowed to run overnight. Brine was then added to quench the reaction and the contents were then transferred to a separatory funnel. Ethyl acetate was used to extract the product and the organic layer was washed with brine (3x). The organic layers were then combined, dried with sodium sulfate and concentrated. The resulting solid was recrystallized in methylene chloride to give yields of 65–80%. The resulting propargyl amides are characterized below.

***N*-(Prop-2-ynyl)-1*H*-pyrrole-2-carboxamide.**  $^1\text{H}$  NMR (400 MHz,  $\text{CD}_3\text{OD}$  at 3.31 ppm)  $\delta$  6.91 (m, 1H), 6.79 (m, 1H), 6.16 (m, 1H), 4.09 (d,  $J = 2.0$  Hz, 2H), 2.56 (t,  $J = 2.2$  Hz, 1H);  $^{13}\text{C}$  NMR (75 MHz,  $\text{CD}_3\text{OD}$ )  $\delta$  163.5, 126.6, 123.3, 112.2, 110.4, 81.2, 72.0, 29.4; HRMS (ESI) calculated for  $\text{C}_8\text{H}_9\text{N}_2\text{O}$  ( $\text{MH}^+$ ) 149.0709, found 149.0708.

**4-Bromo-*N*-(prop-2-ynyl)-1*H*-pyrrole-2-carboxamide.**  $^1\text{H}$  NMR (300 MHz,  $\text{CD}_3\text{OD}$  at 3.31 ppm)  $\delta$  6.92 (s, 1H), 6.78 (s, 1H), 4.08 (d,  $J = 2.1$  Hz, 2H), 2.57 (t,  $J = 2.3$  Hz, 1H);  $^{13}\text{C}$  NMR (75 MHz,  $\text{CD}_3\text{OD}$ )  $\delta$  162.2, 127.3, 123.2, 113.7, 97.6, 81.0, 72.1,

29.4; HRMS (ESI) calculated for  $\text{C}_8\text{H}_8\text{N}_2\text{OBr}$  ( $\text{MH}^+$ ) 225.9742, found 225.9744.

**4,5-Dibromo-*N*-(prop-2-ynyl)-1*H*-pyrrole-2-carboxamide.**  $^1\text{H}$  NMR (400 MHz,  $\text{CD}_3\text{OD}$  at 3.31 ppm)  $\delta$  6.82 (s, 1H), 4.08 (d,  $J = 2.4$  Hz, 2H), 2.58 (t,  $J = 2.7$  Hz, 1H);  $^{13}\text{C}$  NMR (100 MHz,  $\text{CD}_3\text{OD}$ )  $\delta$  161.4, 128.6, 114.7, 106.6, 100.2, 80.9, 72.2, 29.4; HRMS (ESI) calculated for  $\text{C}_8\text{H}_7\text{N}_2\text{OBr}_2$  ( $\text{MH}^+$ ) 304.8919, found 304.8924.

#### Acknowledgements

The authors would like to thank the University of North Carolina General Administration for funding this work.

#### References

- 1 D. J. Musk and P. J. Hergenrother, *Curr. Med. Chem.*, 2006, **13**, 2163.
- 2 R. M. Donlan and J. W. Costerton, *Clin. Microbiol. Rev.*, 2002, **15**, 167.
- 3 A. Adonizio, K.-F. Kong and K. Mathee, *Antimicrob. Agents Chemother.*, 2008, **52**, 198.
- 4 C. M. Waters, W. Lu, J. D. Rabinowitz and B. L. Bassler, *J. Bacteriol.*, 2008, **190**, 2527.
- 5 G. M. Patriquin, E. Banin, C. Gilmour, R. Tuchman, P. E. Greenberg and K. Poole, *J. Bacteriol.*, 2008, **190**, 662.
- 6 T. B. Rasmussen and M. Givskov, *Int. J. Med. Microbiol.*, 2006, **296**, 149.
- 7 G. D. Geske, R. J. Wezeman, A. P. Siegel and H. E. Blackwell, *J. Am. Chem. Soc.*, 2005, **127**, 12762.
- 8 Y. H. Dong and L. H. Zhang, *J. Microbiol.*, 2005, **43**, 101.
- 9 K. H. Nealson, T. Platt and J. W. Hastings, *J. Bacteriol.*, 1970, **104**, 313.
- 10 M. Hentzer, K. Riedel, T. B. Rasmussen, A. Heydorn, J. B. Anderson, M. R. Parsek, S. A. Rice, L. Eberl, S. Molin, N. Hoiby, S. Kjelleberg and M. Givskov, *Microbiology (Reading, UK)*, 2002, **148**, 87.
- 11 J. F. Hu, E. Garo, M. G. Goering, M. Pasmore, H. D. Yoo, T. Esser, J. Sestrich, P. A. Cremin, G. W. Hough, P. Perrone, Y. S. L. Lee, N. T. Le, M. O'Neil-Johnson, J. W. Costerton and G. R. Eldrich, *J. Nat. Prod.*, 2006, **69**, 118.
- 12 L. M. Junker and J. Clardy, *Antimicrob. Agents Chemother.*, 2007, **51**, 3582.
- 13 R. W. Huigens, J. J. Richards, G. Parise, T. E. Ballard, W. Zeng, R. Deora and C. Melander, *J. Am. Chem. Soc.*, 2007, **129**, 6966.
- 14 J. J. Richards, R. W. Huigens, T. E. Ballard, A. Basso, J. Cavanagh and C. Melander, *Chem. Commun.*, 2008, **14**, 1698.
- 15 J. J. Richards, T. E. Ballard and C. Melander, *Org. Biomol. Chem.*, 2008, **6**, 1356.
- 16 R. W. Huigens, L. Ma, C. Gambino, P. D. R. Moeller, A. Basso, J. Cavanagh, D. J. Wozniak and C. Melander, *Mol. Biosyst.*, 2008, **4**, 614.
- 17 J. J. Richards, T. E. Ballard, R. W. Huigens and C. Melander, *ChemBioChem*, 2008, **9**, 1267.
- 18 S. A. Rogers and C. Melander, *Angew. Chem., Int. Ed.*, 2008, **47**, 5229.
- 19 J. J. Richards, C. S. Reed and C. Melander, *Bioorg. Med. Chem. Lett.*, 2008, **18**, 4325.
- 20 A. Yamada, H. Kitamura, K. Yamaguchi, S. Fukuzawa, C. Kamijima, K. Yazawa, M. Kuramoto, G. Y. S. Wang, Y. Fujitani and D. B. Uemura, *Chem. Soc. Jpn.*, 1997, **70**, 3061.
- 21 M. E. Falagas, P. K. Koletsi and I. A. Bliziotis, *J. Med. Microbiol.*, 2006, **55**, 1619.
- 22 S. Shelburn, K. Singh, C. White, L. Byrne, A. Carmer, C. Austin, E. Graviss, C. Stager, B. Murray and R. Atmar, *J. Clin. Microbiol.*, 2008, **46**, 198.
- 23 J. S. Hawley, C. K. Murray, M. E. Griffith, M. L. McElmeel, L. C. Fulcher, D. R. Hospenthal and J. H. Jorgensen, *Antimicrob. Agents Chemother.*, 2007, **51**, 376.
- 24 F. Menichetti, *Clin. Microbiol. Infect.*, 2005, **11**, 22.
- 25 J. W. Costerton, P. S. Stewart and E. P. Greenberg, *Science*, 1999, **284**, 1318.
- 26 P. A. Lambert, *J. R. Soc. Med.*, 2002, **95**, 22.
- 27 P. Wipf, Y. Aoyama and T. E. Benedum, *Org. Lett.*, 2004, **6**, 3593.